Original Article

Distinct iris gene expression profiles of primary angle closure glaucoma and primary open angle glaucoma and their interaction with ocular biometric parameters

Li-Fong Seet PhD,[1,2,3,*] Arun Narayanaswamy MMed,[4,*] Sharon N Finger BSc,[1] Hla M Htoon PhD,[1,3] Monisha E Nongpiur MD PhD,[1,2,3] Li Zhen Toh BSc,[1] Henrietta Ho FRCOphth,[4] Shamira A Perera FRCOphth[1,4] and Tina T Wong FRCSEd PhD[1,2,3,4,5]

[1]Singapore Eye Research Institute, [2]Department of Ophthalmology, Yong Loo Lin School of Medicine, National University of Singapore, [3]Duke-NUS Graduate Medical School, [4]Singapore National Eye Centre and [5]School of Materials Science and Engineering, Nanyang Technological University, Singapore

ABSTRACT

Background: This study aimed to evaluate differences in iris gene expression profiles between primary angle closure glaucoma (PACG) and primary open angle glaucoma (POAG) and their interaction with biometric characteristics.

Design: Prospective study.

Participants: Thirty-five subjects with PACG and thirty-three subjects with POAG who required trabeculectomy were enrolled at the Singapore National Eye Centre, Singapore.

Methods: Iris specimens, obtained by iridectomy, were analysed by real-time polymerase chain reaction for expression of type I collagen, vascular endothelial growth factor (VEGF)-A, -B and -C, as well as VEGF receptors (VEGFRs) 1 and 2. Anterior segment optical coherence tomography (ASOCT) imaging for biometric parameters, including anterior chamber depth (ACD), anterior chamber volume (ACV) and lens vault (LV), was also performed pre-operatively.

Main Outcome Measures: Relative mRNA levels between PACG and POAG irises, biometric measurements, discriminant analyses using genes and biometric parameters.

Results: *COL1A1*, *VEGFB*, *VEGFC* and *VEGFR2* mRNA expression was higher in PACG compared to POAG irises. LV, ACD and ACV were significantly different between the two subgroups. Discriminant analyses based on gene expression, biometric parameters or a combination of both gene expression and biometrics (LV and ACV), correctly classified 94.1%, 85.3% and 94.1% of the original PACG and POAG cases, respectively. The discriminant function combining genes and biometrics demonstrated the highest accuracy in cross-validated classification of the two glaucoma subtypes.

■ **Correspondence:** Dr Li-Fong Seet, Singapore Eye Research Institute, The Academia, 20 College Road, Discovery Tower, #06-98, Singapore 169856. E-mail: seet.li.fong@seri.com.sg and Dr Tina Wong, Singapore National Eye Centre, 11 Third Hospital Avenue, Singapore 168751. E-mail: tina.wong.t.l@snec.com.sg

*LFS and AN contributed equally to this study.

Conclusions: Distinct iris gene expression supports the pathophysiological differences that exist between PACG and POAG. Biometric parameters can combine with iris gene expression to more accurately define PACG from POAG.

Key words: biometrics, iris, PACG, POAG.

INTRODUCTION

The glaucomas are a group of heterogeneous optic neuropathy characterized by progressive degeneration of the retinal ganglion cells. Age and elevated intraocular pressure (IOP) are important risk factors. Recent progress in genome-wide association studies,[1,2] gene expression screening[3] and proteomic analyses[4] have revealed novel genetic risk factors and biomarkers, promising to improve diagnosis and treatment strategies for glaucoma.

Primary glaucoma may be classified into two main categories: primary open-angle glaucoma (POAG) and primary angle-closure glaucoma (PACG). PACG is three times more likely to cause bilateral visual impairment than POAG.[5] Hence, accurate diagnosis is paramount. PACG is associated with several ocular biometric risk factors including well-established factors such as shallow anterior chamber depth (ACD), thick lens and shorter axial length (AL), as well as the recently identified imaging-based factors such as small anterior chamber width, area and volume (ACW, ACA, ACV), thicker iris with greater iris area and curvature, plateau iris configuration and larger lens vault (LV).[6-9] In addition to the above-mentioned anatomical factors, dynamic mechanisms such as altered responses of the iris to pupil dilation and the development of choroidal effusion have been implicated in the pathogenesis of PACG. These mounting observations suggest that altered iris structure and biomechanics may emerge as distinguishing features of PACG.

However, there is limited data pertaining to altered gene expression in glaucoma iris. A study involving iris specimens from Chinese patients suggests relatively higher collagen content in acute angle closure eyes compared to POAG eyes when assessed by sirius red staining.[10] In another study, SPARC (secreted protein, acidic and rich in cysteine) and collagen I transcripts were found to be elevated in PACG compared to POAG iris.[11] SPARC is a matricellular glycoprotein involved in the regulation of collagen deposition.[12] Together, these data strongly suggest elevated collagen level in the iris could be a distinct biological signature for PACG relative to POAG.

Besides collagen, vascular endothelial growth factor (VEGF) is also implicated in glaucoma. VEGF is one of the most potent promoters of angiogenesis.[13] The association between increased VEGF in the aqueous and glaucoma has been reported previously.[14,15] Moreover, a recent study demonstrated correlation between IOP and VEGF levels in the aqueous humour of acute primary angle-closure eyes.[16] In this study, iris tissue from POAG and PACG patients was examined for the expression of genes implicated in glaucoma including *COL1A1*, *VEGF* members *A* to *C*, as well as *VEGFR* members *1* and *2*. Their potential as unique discriminating factors and their interaction with biometric parameters for distinguishing PACG from POAG were also evaluated.

METHODS

Patients

Subjects were recruited from outpatient clinics of the Singapore National Eye Centre (SNEC) between March 2011 and Dec 2012. This study was reviewed and approved by the institutional review and ethics board at the Singapore Eye Research Institute (SERI) and adhered to the tenets of the Declaration of Helsinki. Written informed consent was obtained from all subjects.

Subjects requiring trabeculectomy because of poorly controlled IOP despite maximal medical therapy and/or progressive visual field loss and optic disc cupping were recruited. POAG and PACG were diagnosed in the presence of glaucomatous optic nerve head damage, defined as a vertical cup:disc (CD) ratio of >0.7, CD asymmetry of >0.2 and/or focal notching with corresponding visual field loss on static perimetry (SITA Standard algorithm with a 24–2 test pattern, Humphrey Visual Field Analyzer II: Carl Zeiss Meditec, Dublin, CA). PACG eyes had gonioscopic findings of angle closure, defined as having the posterior trabecular meshwork not visible for at least 180° on non-indentation gonioscopy, with or without peripheral anterior synechiae. Combined trabeculectomy with mitomycin C and cataract surgery was performed where clinically indicated. Subjects with evidence of secondary glaucoma were excluded. Subjects taking medication that have effects on the iris (specifically miotics, mydriatics and systemic tamsulosin) were also excluded.

Iris specimen

Iris tissue from 34 PACG patients and 30 POAG patients were collected for analysis. Iris tissues specimens were obtained from peripheral iridectomies performed as part of a standard trabeculectomy procedure. Peripheral iridectomies were performed between 10 and 2 o'clock of the superior peripheral iris. Iris specimens were collected in RNAlater

solution (Thermo Fisher Scientific Inc, MA, USA) and stored at −80 °C until analyses were performed.

Real-time quantitative polymerase chain reaction (qPCR)

Iris specimens were lysed by sonication and total RNA recovered with Trizol Reagent (Invitrogen Corp, CA, USA) and the RNeasy kit (Qiagen, Valencia, CA) as described previously.[17] Five nanograms of total RNA was reverse-transcribed into cDNA using random hexamer primers (Invitrogen Corp) with Superscript III reverse transcriptase (Invitrogen Corp). All qPCR reactions, comprising the Power SYBR Green PCR Master Mix (Applied BioSystems, CA, USA), were performed in triplicates in volumes of 10 μl in 384-well microtiter plates and run using the Roche LightCycler 480 System (Roche Diagnostics Corp, Indianapolis, USA). All mRNA levels were measured as C_T threshold levels. *ACTB* was used as the housekeeping gene, determined to be the most suitable of four analysed (*ACTB*, *RNA18S1*, *GAPDH*, *RPL13A*) using the NormFinder software.[18] The average ΔC_T value calculated from the POAG irises for each gene was used for calculating the fold change in gene expression in the PACG irises by the $2^{-\Delta\Delta C_T}$ method. Primers used for qPCR are shown in Table 1.

Anterior segment-optical coherence tomography (AS-OCT)

ASOCT imaging was obtained for a total of 20 PACG and 18 POAG patients. AS-OCT was performed using the Visante OCT (Carl Zeiss Meditec AG, Dublin, CA, USA) by a single trained technician using the quad-scan mode, which captures anterior segment images simultaneously along the meridians of 45, 90, 135 and 180°. Subjects were imaged twice, first after dark-adaption (0 lux) for at least 5 min before imaging, followed by repeat imaging whilst continuously exposing the fellow eye to bright light (1700 lux, pen light).

Custom semi-automated software (Zhongshan Angle Assessment Program [ZAAP]) was used to analyse the AS-OCT images.[19] The scleral spur obtained from each image was identified and marked, and the following averages of parameters were generated from the software: iris cross-sectional area, iris volume, anterior chamber width (ACW), anterior chamber area (ACA), anterior chamber volume (ACV) and lens vault (LV). The 90° images were excluded from analysis because of lid artifacts causing poor image quality along that meridian. Average pupil diameter was measured along meridians of 45, 135 and 180°.

Statistical methods

Post-hoc power analysis was performed using the iris gene expression data. The two-sample *t*-test power analysis estimated that group sample sizes of 30 will achieve 96% power to detect a difference of 0.7 between the null hypothesis that two group means are 1.8 and the alternative hypothesis that the mean of group 2 is 1.1 with known group standard deviations of 0.9 and 0.7 and with a significance level (alpha) of 0.05000.

All statistical analyses were performed using the SPSS version 19 software (IBM SPSS Statistics for Windows, Version 19.0. Armonk, NY: IBM Corp. Released 2010.). To compare gene expression or biometric measurements between PACG and POAG irises, the Student's two-tailed *t*-test was used, and the significance of differences between the parameters was

Table 1. Primer sequences for quantitative real-time PCR analysis of human iris tissue

Gene	Accession		Sequences (5′ → 3′)	Length (bp)
ACTB	NM006715764	for	CCAACCGCGAGAAGATGA	18
		rev	CCAGAGGCGTACAGGGATAG	20
COL1A1	NM000088	for	CAGCCGCTTCACCTACAGC	19
		rev	TTTTGTATTCAATCACTGTCTTGCC	25
VEGFA	NM001171623	for	CCTCCGAAACCATGAACTTT	20
		rev	CCACTTCGTGATGATTCTGC	20
VEGFB	NM001243733	for	GATGGCCTGGAGTGTGTG	18
		rev	CACACTGGCTGTGTTCTTCC	20
VEGFC	NM005429	for	GGCTGGCAACATAACAGAGA	20
		rev	GTGGCATGCATTGAGTCTTT	20
VEGFR1	NM002019	for	CGACGTGTGGTCTTACGGAGTA	22
		rev	CTTCCCTCAGGCGACTGC	18
VEGFR2	NM002253	for	TGCCTCAGAAGAGCTGAAAACTT	23
		rev	CACAGACTCCCTGCTTTTGCT	21

All primer sets were used under identical cycling conditions. Sequences were obtained from GenBank and accession numbers are denoted.

corrected by Bonferroni post-hoc adjustment. A *P* value <0.05 was deemed to be statistically significant.

Gene expression (*COL1A1*, *VEGFB*, *VEGFC*, *VEGR2*) or biometric parameters (LV, ACD, ACV) that were significantly different between PACG and POAG were selected as potential predictors for a linear discriminant analysis of these two glaucoma subtypes. To differentiate between PACG and POAG and to potentially define the allocation of new observations into either group using multivariate discriminant analysis, three multivariate models were considered, based on gene expression parameters alone, biometric parameters alone or a combination of both. The discriminant model is based on a few assumptions including multivariate normality, equality of variance–covariance within each group and low multicollinearity of the variables in order to reliably predict group membership. In accordance with these assumptions, gene expression data required normalization by conversion to the natural logarithmic form. Hence, gene expression data, whether analysed alone or in combination with biometric data, were imputed in the discriminant analysis in the natural logarithmic form. To check the assumption of homogeneity of the covariance matrix within each group, Box's M test of equality was used. Multicollinearity of the parameters was examined using correlation analysis, with correlations greater than 0.80 to be excluded.

With the classification of glaucoma types as the outcome, Wilk's Lambda statistic with Chi Square Test was used to test the significance of the model. A classification functional equation was constructed which facilitates the prediction of the glaucoma type based on the value of the classification function. All cases but one cross-validation was performed to determine the accuracy and veracity of the classification function.

RESULTS

A total of 68 subjects were enrolled in the study. 35 subjects were diagnosed with PACG and 33 subjects with POAG. The mean ages of the PACG and POAG groups were 67.3 ± 7.0 and 70.4 ± 9.2 years, respectively (*P* = 1.10). The subjects were predominantly male (63% in PACG and 88% in POAG; *P* = 0.15) and mainly of Chinese ethnicity (77% in PACG and 91% in POAG; *P* = 2.37). Amongst the PACG subjects, the iris tissues of 34 were analysed for gene expression and ASOCT measurements were available for 20 eyes. The total number of PACG subjects analysed for both gene expression and biometric parameters was 19. For POAG, the iris tissues from 30 subjects were measured for gene expression and ASOCT was available for 18 subjects. The total number of POAG subjects with both gene expression and biometric data 15.

Differential gene expression between PACG and POAG

Iris tissues from PACG and POAG subjects were analysed for mRNA expression of *COL1A1*, *VEGFA*, *VEGFB*, *VEGFC*, *VEGFR1* and *VEGFR2* by quantitative real-time PCR (Fig. 1). Data from the POAG iris were used as baseline values for comparisons of fold changes in gene expression in PACG irises. Between the two glaucoma subtypes, PACG irises expressed significantly higher levels of *COL1A1*, *VEGFB*, *VEGFC* and *VEGFR2* transcripts compared to POAG irises (Fig. 1).

Differential biometric characteristics between PACG and POAG

The ASOCT-based biometric parameters that were evaluated include ACD, ACW, ACV, LV, iris area, iris volume and pupil diameter. PACG subjects demonstrated significantly larger LV with smaller ACD and ACV compared to POAG subjects, irrespective of lighting conditions (Fig. 2). The other parameters measured were not significantly different between the two glaucoma subtypes (data not shown).

Discriminant analyses of PACG and POAG using iris gene expression and biometric parameters

Given that there are parameters in both gene expression (*COL1A1*, *VEGFB*, *VEGFC* and *VEGFR2*), and biometric measurements (LV, ACD and ACV) that were significantly different between PACG and POAG, we proceeded to use discriminant analyses to test if gene expression parameters would effectively differentiate PACG from POAG as compared to differentiation using known biometric parameters. For a fair comparison of the discriminant functions utilizing genes alone, biometrics alone or a combination of both, we analysed data from patients who have been evaluated for both set of parameters, that is, 19 PACG and 15 POAG subjects.

To test for gene expression parameters alone, the fold change values were first normalized by conversion to natural logarithm. The resulting discriminant function accounted for 62.57% of the total variability. The box plot of the discriminant function demonstrated clear separation in the distribution of the discriminant function scores for PACG and POAG (Fig. 3a). *COL1A1* expression was the strongest predictor (Table 2). The classification results revealed that 94.1% of the original cases were classified correctly into PACG and POAG groups, whilst cross-validated classification revealed that overall, 88.2% of cases were classified correctly (Table 3).

Next, the effectiveness of biometric parameters to differentiate between PACG and POAG was evaluated.
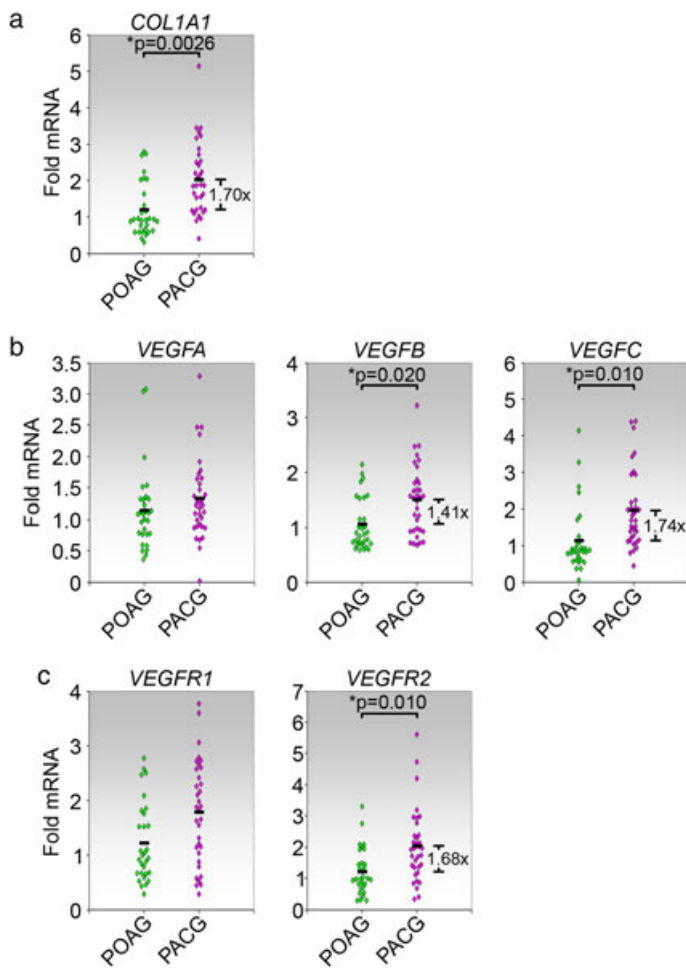
Figure 1. Gene expression in the irises of PACG and POAG patients. The irises of 34 PACG and 30 POAG patients were analysed for mRNA expression of (A) type I collagen (*COL1A1*), (B) VEGFs (*VEGFA*, *VEGFB*, *VEGFC*) and (C) VEGF receptors (*VEGFR1*, *VEGFR2*). Significant fold changes in PACG relative to POAG and the associated *P* values (*) are indicated. Each symbol represents one patient.
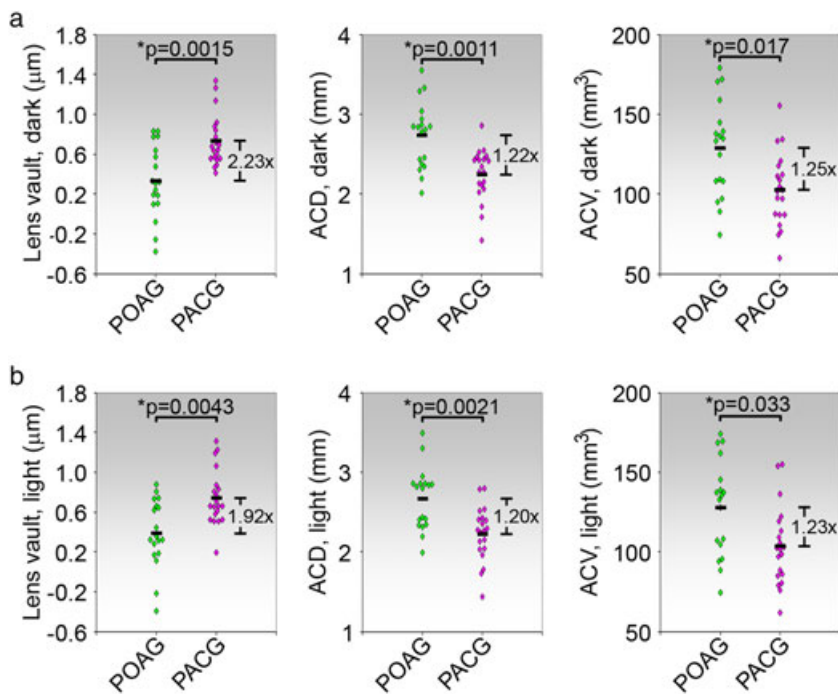

Figure 2. The biometric measurements of ACD, ACV and LV are significantly different between PACG and POAG patients. 20 PACG and 18 POAG patients were measured by AS-OCT in both dark (A) and illuminated (B) conditions. The values for the fold changes between PACG and POAG biometric parameters and the respective *P* values for the comparisons are indicated.

The resulting discriminant function accounted for 43.56% of the variation, with ACD being the strongest predictor (Table 2). 85.3% of the original cases were classified correctly into PACG and POAG groups (Table 3). The box plot revealed decreased segregation in the discriminant function scores compared to that
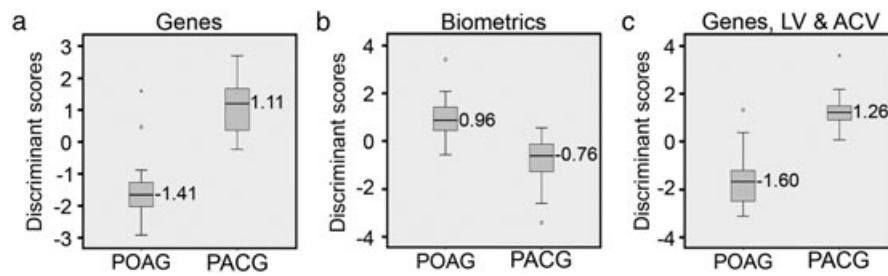
Figure 3. Box plots for the discriminant functions based on (A) gene expression of *COL1A1*, *VEGFB*, *VEGFC* and *VEGFR2*, (B) biometric measurements (LV, ACD, ACV) and (C) a combination of gene expression (*COL1A1*, *VEGFB*, *VEGFC* and *VEGFR2*) and biometric measurements (LV and ACV). Numbers indicate the group means of the respective discriminant functions.

Table 2. Standardized canonical coefficients from linear discriminant analysis and comparison of discriminant functions

Variables	Function: genes only PACG ($n=19$) POAG ($n=15$)		Function: biometrics only PACG ($n=19$) POAG ($n=15$)		Function: genes & biometrics (LV and ACV) PACG ($n=19$) POAG ($n=15$)	
	Standardized coefficient	Relative importance	Standardized coefficient	Relative importance	Standardized coefficient	Relative importance
COL1A1	0.606	0.876	—	—	0.541	0.773
VEGFB	0.136	0.772	—	—	0.060	0.681
VEGFR2	0.400	0.744	—	—	0.340	0.656
VEGFC	0.304	0.219	—	—	0.422	0.193
ACD, dark	—	—	2.571	0.831	—	—
LV, dark	—	—	0.002	−0.830	0.769	0.498
ACV, dark	—	—	−1.825	0.622	0.391	−0.373
Eigenvalue	1.670		0.774		2.148	
Proportion of trace (%)	62.57		43.56		68.23	
Significance	<0.001		<0.01		<0.001	
Correct classification (original) (%)	94.1		85.3		94.1	
Correct classification (cross-validated) (%)	88.2		70.6		91.2	

Genes only indicates the inclusion of *COL1A1*, *VEGFB*, *VEGFC* and *VEGFR2* expression data in the discriminant analysis. Biometrics only indicates the inclusion of lens vault (LV), anterior chamber depth (ACD) and anterior chamber volume (ACV) in the discriminant analysis. Standardized coefficient: standardized coefficient obtained from the linear discriminant analysis of each variable for the indicated functions. Proportion of trace (%): proportion of variability of the outcome explained by the indicated variables.

based on gene expression parameters (Fig. 3b). Hence, biometric parameters alone provided less accurate grouping of PACG and POAG compared to gene expression parameters.

We next assessed the performance of the discriminant function that incorporates both gene expression and biometric data. Because ACD and ACV are related measures, discriminant functions for each of the combinations consisting of the expression of the four genes and LV with either ACD or ACV were analysed. We found that the discriminant function consisting of gene expression, LV and ACV produced the best differentiation and accounted for the highest % of variability (eigenvalue = 2.148, proportion of trace = 68.23%) compared with the function consisting of gene expression, LV and ACD (eigenvalue = 2.066, proportion of trace = 67.40%). The

structure matrix for the discriminant function incorporating genes, LV and ACV as parameters, revealed that gene expression was generally stronger predictors compared to LV or ACV, with the exception of *VEGFC* (Table 2); 94.1% of the original cases were classified correctly into PACG and POAG, and cross-validated classification was 91.2% accurate (Table 3). The box plot of the discriminant function demonstrated clear segregation of the discriminant function scores (Fig. 3c). Moreover, the AUC (area under the ROC curve) for the discriminant scores of the combined variables was 98.6% (95% CI: 95.4–100, $P < 0.001$), strongly supporting the effectiveness of this discriminant function to distinguish PACG from POAG.

Taken together, iris gene expression profile of *COL1A1*, *VEGFB*, *VEGFC* and *VEGFR2* can discriminate

Table 3. Distribution of predicted versus actual glaucoma subtype classification using discriminant functions generated with gene and/or biometric parameters

Function		Glaucoma subtype	Predicted diagnosis		Number of patients
			PACG	POAG	
Genes only	Original	PACG	19 (100)	0 (0)	19
		POAG	2 (13.3)	13 (86.7)	15
	Cross-validated	PACG	17 (89.5)	2 (10.5)	19
		POAG	2 (13.3)	13 (86.7)	15
Biometrics only	Original	PACG	17 (89.5)	2 (10.5)	19
		POAG	3 (20)	12 (80)	15
	Cross-validated	PACG	15 (78.9)	4 (21.1)	19
		POAG	3 (20)	12 (80)	15
Genes and biometrics (LV, ACV)	Original	PACG	19 (100)	0 (0)	19
		POAG	2 (13.3)	13 (86.7)	15
	Cross-validated	PACG	18 (94.7)	1 (5.3)	19
		POAG	2 (13.3)	13 (86.7)	15

Genes only indicates the inclusion of *COL1A1*, *VEGFB*, *VEGFC* and *VEGFR2* expression data in the discriminant analysis. Biometrics only indicates the inclusion of lens vault (LV), anterior chamber depth (ACD) and anterior chamber volume (ACV) in the discriminant analysis.

between PACG and POAG. However, a combination of both gene expression and biometric data, specifically LV and ACV, generated more effective cross-validated differentiation of PACG from POAG compared to the application of either forms of measurement alone. These data therefore support the division of PACG and POAG as distinct subtypes, characterized not only by established biometric differences, but also by fundamental iris gene expression disparities.

DISCUSSION

This study is the first to report fundamental differences at the molecular level in the glaucomatous PACG and POAG irises. We described in this study that transcript expression of *COL1A1*, *VEGFB*, *VEGFC* and *VEGFR2* was distinct between PACG and POAG irises. Moreover, our data augmented the subgrouping of angle closure based on recently described quantitative ASOCT parameters.[20] Hence, delineating the molecular disparities between glaucoma phenotypes is important for not only contributing to our understanding of disease aetiology/pathogenesis but also for clearer definition of disease subgroups.

Uncovering the underlying molecular bases that differentiates PACG from POAG will refine our understanding of the pathophysiology for the deviation of the two disease processes. However, this is complicated by genetic heterogeneity associated with all forms of glaucoma. Many chromosomic loci have been associated with PACG and POAG, but few are well characterized. A recent genome-wide association analysis identified variants in *COL11A1*, amongst others, as a risk factor for PACG.[21] Loci identified in relation to the risk of POAG include *CDKN2B-AS1*, *TGFBR3-CDC7* and *FNDC3B*, all potentially contributing to the regulation of transforming growth factor-β (TGF-β) signalling. Since TGF-β signalling is involved in a myriad of biological processes, including fibrosis,[22] angiogenesis[23] and lymphangiogenesis,[24] these processes are therefore implicated in the pathogenesis of PACG and/or POAG. Considering that type I collagen is a major profibrotic protein whilst VEGFs, and their cognate receptors, are well established to be involved in angiogenesis and lymphangiogenesis, our findings support the involvement of these biological processes in glaucoma pathogenesis.

The importance of type I collagen in the glaucoma iris, whose expression was prominently different between the two subtypes, is implied in clinical observations of the diseases. For instance, fibrovascular scarring at the anterior chamber angle was a notable feature of IOP-induced ocular damage.[25] This scarring effect may have its origins in the organization of collagen as intimately interwoven fibres with blood vessels in the iris,[26–30] and its synthesis being intimately associated with the activation of these vessels.[27,29] Indeed, VEGFB has been shown to upregulate collagen genes in vascular cells.[31] Furthermore, altered iris mobility in PACG has been described, including reduced loss in iris area consistently observed in angle closure eyes in response to mydriasis compared to open angle or normal eyes[32–34] as well as the slower speed of pupil constriction in PACG eyes.[35] The underlying explanation may be that collagen fibres are major components of the relatively inextensible connective tissue scaffold in the iris.[30] Increased type I collagen in the PACG iris may render it more rigid, thus reducing its ability to stretch and compromising pupil mobility. Gene expression variations, fundamental to tissue dysfunction in diseases, may therefore be vital for

understanding the presentation, pathogenesis and progression of glaucoma subtypes.

Elevated IOP has been linked to ocular ischemia as well as iris stromal necrosis in independent studies.[36,37] We postulate that these phenomena are related and damage to the iris in turn leads to the induction of a tissue repair phenotype in this tissue in glaucoma. The hypoxia accompanying ischemia is known to induce the transcription factor hypoxia-inducible factor-1 (HIF-1) which triggers many processes important for tissue repair by regulating the expression of diverse genes, including VEGF and type I collagen.[38] Whilst the role of collagen in tissue repair is well established,[39] we speculate that the upregulation of *VEGFB* may be a compensatory mechanism to preserve the vasculature of the ischemic glaucoma iris so as to prevent further damage.[40] Hence, the higher transcript expression of collagen and VEGF genes in the PACG iris may potentially indicate greater ischemia and a higher level of hypoxia in PACG compared to POAG, which may in turn explain the poorer prognosis of PACG versus POAG.[5,41]

The significance of the gene expression data suggests that a larger number of subjects for simultaneous tissue and biometric analyses is warranted to further increase the veracity of the conclusion drawn here. A caveat in this study is the assumption that the iris specimen from the superior quadrant is representative of the whole iris. It is also not clear whether the close vicinity of the site where laser iridotomies are performed in the PACG iris may have an influence on the local iris gene expression profile. Future studies involving other independent measures such as determination of VEGFB and VEGFC protein levels in glaucomatous eyes will help to verify the distinct molecular phenotypes that exist between the disease subgroups.

In conclusion, we report distinct gene expression profiles in the POAG and PACG irises which not only distinguished the two subtypes, but also enhanced the accuracy of their description when combined with known biometric characteristics. This study therefore provides evidence to support the importance of understanding the molecular differences between glaucoma phenotypes.

ACKNOWLEDGEMENTS

REFERENCES

1. Vithana EN, Khor CC, Qiao C, *et al.* Genome-wide association analyses identify three new susceptibility loci for primary angle closure glaucoma. *Nat Genet* 2012; **44**: 1142–6.
2. Mackey DA, Hewitt AW. Genome-wide association study success in ophthalmology. *Curr Opin Ophthalmol* 2014; **25**: 386–93.
3. Jakobs TC. Differential gene expression in glaucoma. *Cold Spring Harb Perspect Med* 2014; **4**: a020636.
4. Tezel G. A proteomics view of the molecular mechanisms and biomarkers of glaucomatous neurodegeneration. *Prog Retin Eye Res* 2013; **35**: 18–43.
5. Foster PJ, Johnson GJ. Glaucoma in china: how big is the problem? *Brit J Ophthalmol* 2001; **85**: 1277–82.
6. Sakai H, Morine-Shinjyo S, Shinzato M, Nakamura Y, Sakai M, Sawaguchi S. Uveal effusion in primary angle-closure glaucoma. *Ophthamol* 2005; **112**: 413–9.
7. Lavanya R, Wong TY, Friedman DS, *et al.* Determinants of angle closure in older Singaporeans. *Arch Ophthalmol* 2008; **126**: 686–91.
8. Nongpiur ME, He M, Amerasinghe N, *et al.* Lens vault, thickness, and position in Chinese subjects with angle closure. *Ophthalmol* 2011; **118**: 474–9.
9. Wang BS, Narayanaswamy A, Amerasinghe N, *et al.* Increased iris thickness and association with primary angle closure glaucoma. *Br J Ophthalmol* 2011; **95**: 46–50.
10. He M, Lu Y, Liu X, Ye T, Foster PJ. Histologic changes of the iris in the development of angle closure in Chinese eyes. *J Glaucoma* 2008; **17**: 386–92.
11. Chua J, Seet L, Jiang Y, *et al.* Increased SPARC expression in primary angle closure glaucoma iris. *Mol Vis* 2008; **14**: 1886–92.
12. Bradshaw AD. The role of SPARC in extracellular matrix assembly. *J Cell Commun Signal* 2009; **3**: 239–46.
13. Ferrara N, Bunting S. Vascular endothelial growth factor, a specific regulator of angiogenesis. *Curr Opin Nephrol Hypertens* 1996; **5**: 35–44.
14. Hu DN, Ritch R, Liebmann J, Liu Y, Cheng B, Hu MS. Vascular endothelial growth factor is increased in aqueous humor of glaucomatous eyes. *J Glaucoma* 2002; **11**: 406–10.
15. Li Z, Van Bergen T, Van de Veire S, *et al.* Inhibition of vascular endothelial growth factor reduces scar formation after glaucoma filtration surgery. *Invest Ophthalmol Vis Sci* 2009; **50**: 5217–25.
16. Huang W, Chen S, Gao X, *et al.* Inflammation-related cytokines of aqueous humor in acute primary angle-closure eyes. *Invest Ophthalmol Vis Sci* 2014; **55**: 1088–94.
17. Seet LF, Finger SN, Chu SW, Toh LZ, Wong TT. Novel insight into the inflammatory and cellular responses following experimental glaucoma surgery: a roadmap for inhibiting fibrosis. *Curr Mol Med* 2013; **13**: 911–28.
18. Andersen CL, Jensen JL, Orntoft TF. Normalization of real-time quantitative reverse transcription-PCR data, a model-based variance estimation approach to identify genes suited for normalization, applied to bladder and colon cancer data sets. *Cancer Res* 2004; **64**: 5245–50.
19. Console J, Sakata L, Aung T, Friedman DS, He M. Quantitative analysis of anterior segment optical coherence tomography images: the Zhongshan Angle Assessment Program. *Br J Ophthalmol* 2008; **92**: 1612–6.

20. Nongpiur ME, Gong T, Lee HK, *et al.* Subgrouping of primary angle-closure suspects based on anterior segment optical coherence tomography parameters. *Ophthalmol* 2013; **120**: 2525–31.

21. Vithana EN, Khor CC, Qiao C, *et al.* Genome-wide association analyses identify three new susceptibility loci for primary angle closure glaucoma. *Nat Genet* 2012; **44**: 1142–6.

22. Walraven M, Gouverneur M, Middelkoop E, Beelen RH, Ulrich MM. Altered TGF-β signaling in fetal fibroblasts: what is known about the underlying mechanisms? *Wound Repair Regen* 2014; **22**: 3–13.

23. van Meeteren LA, Goumans MJ, ten Dijke P. TGF-β receptor signaling pathways in angiogenesis; emerging targets for anti-angiogenesis therapy. *Curr Pharm Biotechnol* 2011; **12**: 2108–20.

24. James JM, Nalbandian A, Mukouyama YS. TGFβ signaling is required for sprouting lymphangiogenesis during lymphatic network development in the skin. *Development* 2013; **140**: 3903–14.

25. Anderson DR, Davis EB. Sensitivities of ocular tissues to acute pressure-induced ischaemia. *Arch Ophthalmol* 1975; **93**: 267–74.

26. Konstas AG, Marshall GE, Lee WR. Immunocytochemical localisation of collagens (I–V) in the human iris. *Graefes Arch Clin Exp Ophthalmol* 1990; **228**: 180–6.

27. Wang J, Lin WL, Essner E, Shichi H, Yelian FD. Ultrastructural and immunocytochemical studies of iris vessels in rats with experimental autoimmune uveroretinitis. *Curr Eye Res* 1994; **13**: 747–54.

28. Wang J, Essner E, Shichi H. Tissue repair in the iris in experimental autoimmune uveoretinitis. *Exp Mol Pathol* 1995; **63**: 41–51.

29. Khalil AK, Kubota T, Tawara A, Inomata H. Early changes in iris blood vessels in exfoliation syndrome. *Curr Eye Res* 1998; **17**: 1124–34.

30. Wyatt HJ. A 'minimum-wear-and-tear' meshwork for the iris. *Vis Res* 2000; **40**: 2167–76.

31. Zhang F, Tang Z, Hou X, *et al.* VEGF-B is dispensable for blood vessel growth but critical for their survival, and VEGF-B targeting inhibits pathological angiogenesis. *Proc Natl Acad Sci U S A* 2009; **106**: 6152–7.

32. Quigley HA, Silver DM, Friedman DS, *et al.* Iris cross-sectional area decreases with pupil dilation and its dynamic behavior is a risk factor in angle closure. *J Glaucoma* 2009; **18**: 173–9.

33. Aptel F, Denis P. Optical coherence tomography quantitative analysis of iris volume changes after pharmacologic mydriasis. *Ophthalmol* 2010; **117**: 3–10.

34. Ganeshrao S, Mani B, Ulganathan S, Shantha B, Vijaya L. Change in iris parameters with physiological mydriasis. *Optom Vis Sci* 2012; **89**: 483–8.

35. Zheng C, Cheung CY, Narayanaswamy A, *et al.* Pupil dynamics in Chinese subjects with angle closure. *Graefes Arch Clin Exp Ophthalmol* 2012; **250**: 1353–9.

36. Comez AT, Cakir DU, Tutunculer FK, *et al.* Relationship between raised intraocular pressure and ischemia-modified albumin in serum and humor aqueous: a pilot study in rabbits. *Int J Ophthalmol* 2014; **7**: 421–5.

37. Anderson DR, Davis EB. Sensitivities of ocular tissues to acute pressure-induced ischaemia. *Arch Ophthalmol* 1975; **93**: 267–74.

38. Lokmic Z, Musyoka J, Hewitson TD, Darby IA. Hypoxia and hypoxia signaling in tissue repair and fibrosis. *Int Rev Cell Mol Biol* 2012; **296**: 139–85.

39. Maquart FX, Monboisse JC. Extracellular matrix and wound healing. *Pathol Biol* 2014; **62**: 91–5.

40. Zhang F, Tang Z, Hou X, *et al.* VEGF-B is dispensable for blood vessel growth but critical for their survival, and VEGF-B targeting inhibits pathological angiogenesis. *Proc Natl Acad Sci U S A* 2009; **106**: 6152–7.

41. Gazzard G, Foster PJ, Devereux JG, *et al.* Br J Intraocular pressure and visual field loss in primary angle closure and primary open angle glaucomas. *Ophthalmol* 2003; **87**: 720–5.